The effect of twinning and detwinning on the mechanical property of AZ31 extruded magnesium alloy during strain-path changes

Lifei Wang [a,c], Guangsheng Huang [a,*], Quan Quan [a], Paola Bassani [b], Ehsan Mostaed [c], Maurizio Vedani [c], Fusheng Pan [a]

[a] College of Materials Science and Engineering, Chongqing University, Chongqing 400045, China
[b] Institute for Energetics and Interphases, National Research Council, 23900 Lecco, Italy
[c] Department of Mechanical Engineering, Politecnico di Milano, 20156 Milan, Italy

Article history:
Received 7 April 2014
Accepted 27 May 2014
Available online 18 June 2014

1. Introduction

Magnesium and its alloys have been attracted by large number of industrial sectors due to their low density, high specific strength, high stiffness and good machinability [1,2]. However, owing to the hexagonal close packed (HCP) crystal structure, it exhibits a poor formability at room temperature. That is, there are limited numbers of available slip systems at low temperatures so as the only activated are two basal planes which cannot meet the Mises Criterion addressing which requires 5 independent slip systems [3,4]. As well known, twinning plays an important role at low temperatures for coordinating the deformation along prismatic directions [5]. Moreover, it is well accepted that the {10−12} extension twins could be only generated by loading along the special directions (compression perpendicular to *c*-axis or tension parallel to *c*-axis) [6,7]. Improving the properties of magnesium through exploiting twinning has been widely investigated and a pre-strain has been recognized. Song et al. [8] reported a marked enhancement in tensile and compressive properties of AZ31 plates by pre-rolling along TD whereby grains were divided by the {10−12} twinning lamellae. Xin et al. [9] also reported that the grains could be refined by {10−12} twins generated by pre-compression along the rolling direction, giving rise to improvement of yield and ultimate tensile strength along the transverse direction. Zhang et al. [10] reported that the formability was improved by pre-stretch and annealing through the weakening of basal texture. Besides, detwinning behavior through pre-strain has been also researched aimed at improving the mechanical properties of magnesium alloys. Wang et al. [11] indicated that the yield strength decreased when inverse tension after pre-compression was applied on AZ31 magnesium alloy due to the twinning–detwinning. He et al. [12] also reported that the yield asymmetry of AZ31 magnesium alloy could be effectively controlled by appropriate pre-compression.

Recently, the effect of pre-strain on properties of magnesium alloys has been explored by several researchers [8–12]. However, the inverse deformation after pre-strain, especially pre-stretch, has rarely been considered. In addition, although several researches have concerned the twinning–detwinning effects from fatigue point of view, the aforementioned phenomenon has not been individually addressed. Accordingly, the present study aims the effect of twinning and detwinning during strain-path changes on the mechanical properties of AZ31 magnesium alloy.

2. Experimental procedure

The material used in this work was a commercial AZ31 (Mg–3 wt.%Al–1 wt.%Zn) magnesium alloy in the form of extruded

* Corresponding author. Tel.: +86 23 65112239; fax: +86 23 65102821.
E-mail address: Gshuang@cqu.edu.cn (G. Huang).

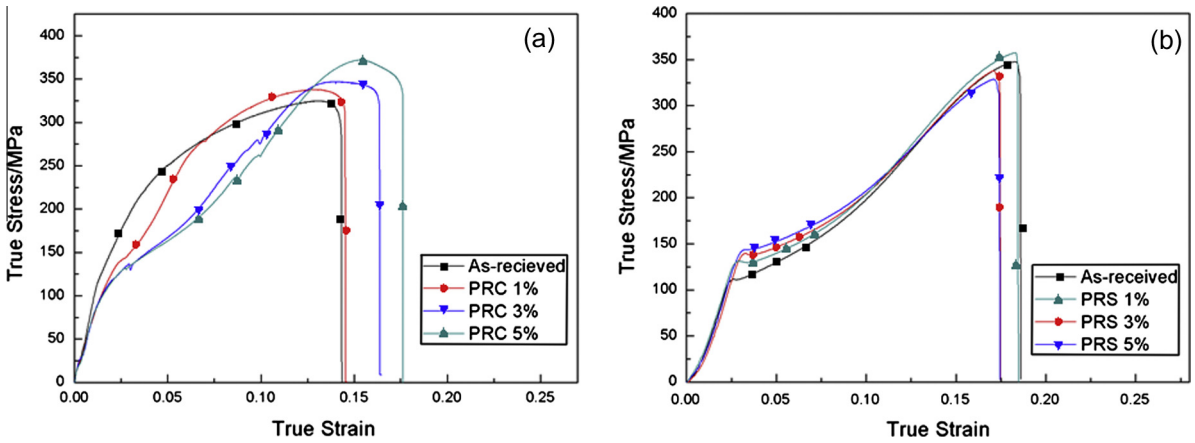

Fig. 1. Stress vs. strain curves: (a) inverse tension after pre-compression and (b) inverse compression after pre-stretch.

bars with a diameter of 16 mm. The AZ31 bars were first annealed at 673 K for 4 h. In order to achieve a microstructure with {10−12} extension twins, some of the bars were pre-compressed along extrusion direction (ED). The levels of the pre-compression were 1%, 3% and 5%, followed by an annealing at 473 K for 2 h aiming at removing excess dislocations and keeping twinning variants. Song et al. [8] reported that the twinning variants were kept in the microstructure even after annealing at 473 K. According to General Administration of Quality Supervision, Inspection and Quarantine of the People's Republic of China (AQSIQ) Standard GB/T 2 28-2002 [13], as-received and pre-compressed bars were cut into dumbbell-shaped tension specimens with nominal gage dimensions of 6 mm × 36 mm. The inverse tension tests were conducted on a CMT6305-300 KN electro-mechanical universal testing machine at room temperature. The strain rate was set at 10^{-3} s^{-1}. Each test was repeated three times.

Another set of bars were pre-stretched along ED at different deformation degrees of 1%, 3% and 5%. Afterwards, annealing at 473 K for 2 h was applied to remove the excess dislocations. Based on General Administration of Quality Supervision, Inspection and Quarantine of the People's Republic of China (AQSIQ) Standard GB/T 7314-2005[14], the pre-stretched bars with height and diameter of 15 mm and 10 mm were cut for compression tests with height and diameter of 15 mm and 10 mm, respectively. Inverse compressive tests were conducted with a strain rate of 10^{-3} s^{-1} at room temperature. Each test was repeated three times.

The microstructure of the alloy before and after the deformation was characterized by optical microscopy and electron backscatter diffraction (EBSD). The microstructure was observed by standard metallographic technique while samples for EBSD observations were prepared by mechanical grinding followed by polishing down to colloidal silica naps. Then electro-polishing was performed using a solution of 20% nitric acid and 80% methanol with a voltage of 20 V for 120 s at temperature −30 °C. Finally, EBSD measurements were performed on a Zeiss EVO 50 SEM. The EBSD data were processed by an INCA OXFORD crystal software.

3. Results and discussions

3.1. Mechanical properties of pre-stretched and pre-compressed samples

True stress–strain curves of inverse tensile tests on pre-compressed specimens and inverse compressive tests on pre-stretched specimens at room temperature are given in Fig. 1. The tensile curves of pre-compressed samples exhibit a concave shape, which is different from the as-received one, suggesting a different deformation mechanism during inverse tension. Mechanical properties derived from the curves in Fig. 1(a and b) are also listed in Table 1, as shown, the yield strength of the as-received alloy was 132 MPa and it decreased to 100, 97 and 94 MPa for PRC 1%, PRC 3% and PRC 5% samples, respectively. The peak strength (PS) values of the PRC samples seemed to be much higher than samples without PRC. Moreover, fracture elongations of all PRC samples were also slightly higher than that of the as-received one.

Table 1
Yield strength (YS), Peak strength (PS), fracture elongation (FE) of various samples along the ED.

		YS/MPa	PS/MPa	FE/%
Pre-compression then tension	As-received	132 ± 4	323 ± 3	12.7 ± 0.2
	PRC 1%	100 ± 2	333 ± 2	12.9 ± 0.3
	PRC 3%	97 ± 3	345 ± 4	14.6 ± 0.3
	PRC 5%	94 ± 2	370 ± 3	16.1 ± 0.2
Pre-stretch then compression	As-received	108 ± 4	349 ± 3	18.6 ± 0.4
	PRS 1%	128 ± 3	347 ± 2	18.2 ± 0.3
	PRS 3%	137 ± 3	337 ± 4	17.4 ± 0.2
	PRS 5%	148 ± 2	325 ± 3	17.2 ± 0.3

Fig. 1(b) represents the mechanical response under inverse compression along ED in pre-stretched samples. As seen, the samples without pre-stretch (as received alloy) showed a clear yield plateau, typical feature of {10−12} extension twinning [15,16]. Similar yield plateaus also appeared in all the curves of the pre-stretched (PRS) samples, implying that the dominant deformation mechanism during inverse compression along ED was still twinning and no changes arose from PRS. Compared with samples without PRS, the yield stress increased significantly in PRS samples. The gain was about 20, 29 and 40 MPa in PRS 1%, PRS 3% and PRS 5%, respectively. Concurrently, the peak strength was slightly reduced after the different PRS degree.

3.2. Microstructure of pre-compressed samples

The microstructure and pole figures of as-received, PRC specimens as well as the schematic view of the orientation of grains after PRC are shown in Fig. 2. The as received sample revealed a nearly equiaxial microstructure exhibiting ⟨0001⟩ fiber texture, with a grain size of about 15.5 μm (Fig. 2a). However, as PRC proceeded, large amount of twins progressively were introduced in the samples' microstructures. According to the EBSD map, the boundaries of twinning lamella were {10−12} extension twinning boundaries. Due to the {10−12} extension twins, the grains

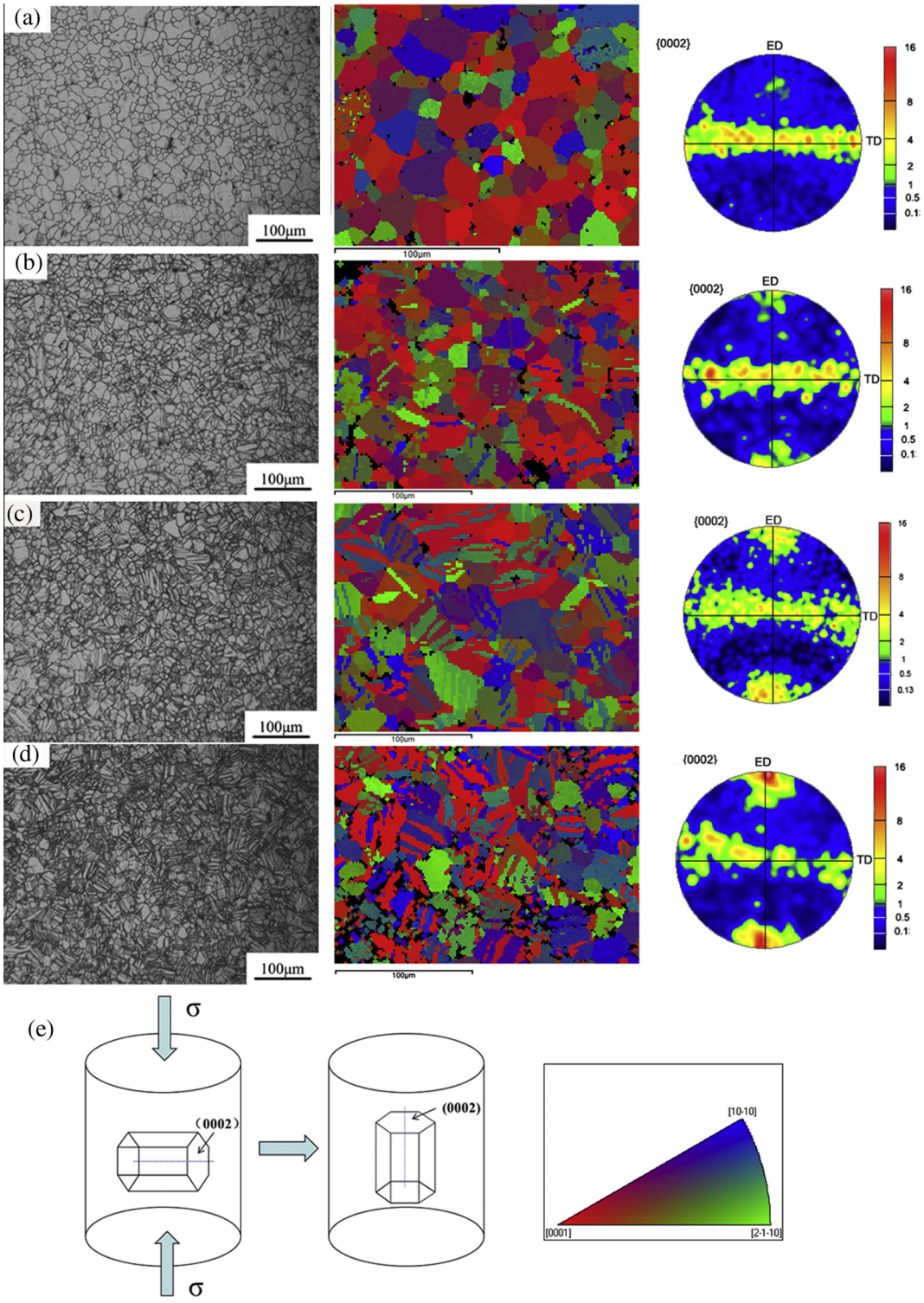

Fig. 2. The microstructure and (0002) pole figures of AZ31 magnesium alloy along cross section: (a) as-received, (b) PRC 1%, (c) PRC 3%, (d) PRC 5% and (e) schematic diagram of orientations of grains after PRC.

preferentially were rotated by about 86°, leading to a *c*-axis ||ED texture. With the increase of PRC levels, more grains oriented close to ED, producing a stronger twinning texture, as shown in Fig. 2. The volume fraction of the twins in PRC 1%, PRC 3%, PRC 5% samples were 18.2%, 26.5% and 36.9%, respectively.

Lou et al. [17] indicated that the twins had a function of refining grains. In PRC 5%, many grains were nearly entirely twinned, leaving only small volumes of untwinned matrix. Thus, the grain refinement effect was more pronounced in PRC 5%. For as-received AZ31 extruded magnesium alloy, the orientation of the grains was perpendicular to the extrusion axis. However, as shown in Fig. 2(e), after PRC the crystal lattices were rotated by 86°, nearly parallel to the extrusion axis.

The optical micrographs of AZ31 magnesium alloy after inverse tension in as-received, PRC 1%, PRC 3% and PRC 5% samples are shown in Fig. 3. As observed, inverse tension in pre-compressed

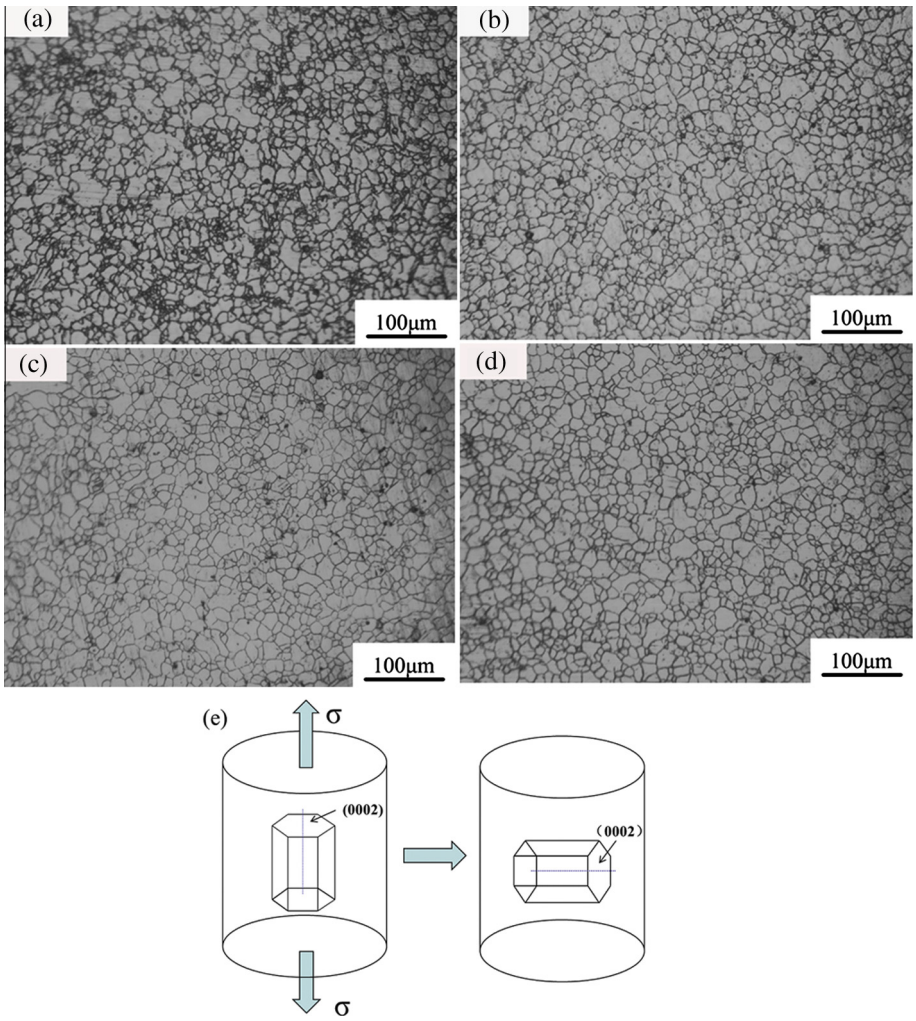

Fig. 3. The optical microstructure of AZ31 Magnesium alloy inverse tension fracture: (a) as-received, (b) PRC 1%, (c) PRC 3%, (d) PRC 5% and (e) schematic diagram of orientations of grains after inverse tension.

specimens led to detwinning occurrence. Simply put, all the twinning lamella disappeared and an equiaxial grain distribution became visible in the microstructure. Wu et al. [18] indicated that the detwinning behavior happened when the load was applied in the inverse direction Fig. 2(e) schematically depicts that in the as extruded alloy most of the basal planes are nearly parallel to ED; however, pre-compression causes the reorientation of those planes by almost 90°. When a reverse stress was applied along ED, the orientation of the twinned regions became favorable for twinning owing to tensile load applied along the *c*-axis of the hexagonal unit cells. Therefore, detwinning occurred in inverse tension process and the crystals reoriented by almost 86° with the basal again parallel to ED, as shown in Fig. 3(e). He et al. [12] found the same phenomenon and confirmed it by XRD. After pre-compression the (0002) diffraction peak increased, while after inverse tension (0002) and (10–10) diffraction peaks decreased and increased, respectively. Due to the occurrence of detwinning, the yield stress of the pre-compressive samples dropped. This phenomenon was consistent with the results given in Table 1 and plotted in the curves of Fig. 1(a). Although detwinning was very similar to the twinning process, the detwinning mechanism may require less stress to be activated because of the already existed twins in the microstructure whereby no nucleation is needed. In addition, back-stresses engendered by the twinning growth may aid the detwinning process [19]. Hence, it can be inferred that detwinning leads to a lower yield strength value.

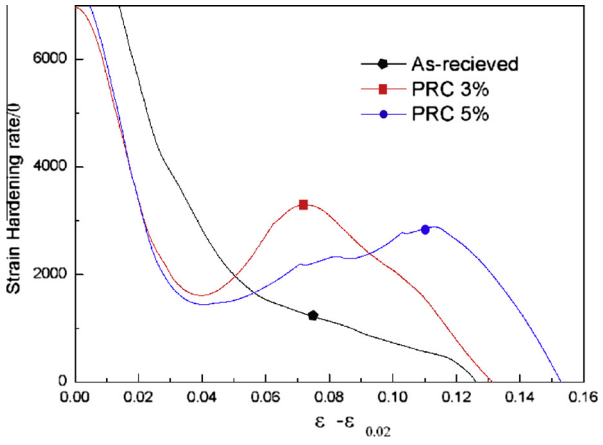

Fig. 4. Strain hardening rate as a function of tensile strain for samples subjected to different compressive pre-compression.

Because of the occurrence of de-twinning, the yield stresses of the samples subjected to PRC 3% and PRC 5% are almost equal. This behavior suggests that the yield stress was mainly controlled by the activation of {10−12} twinning when tensile stress acted along *c*-axis [12]. However, as shown in Fig. 1(a), a big difference

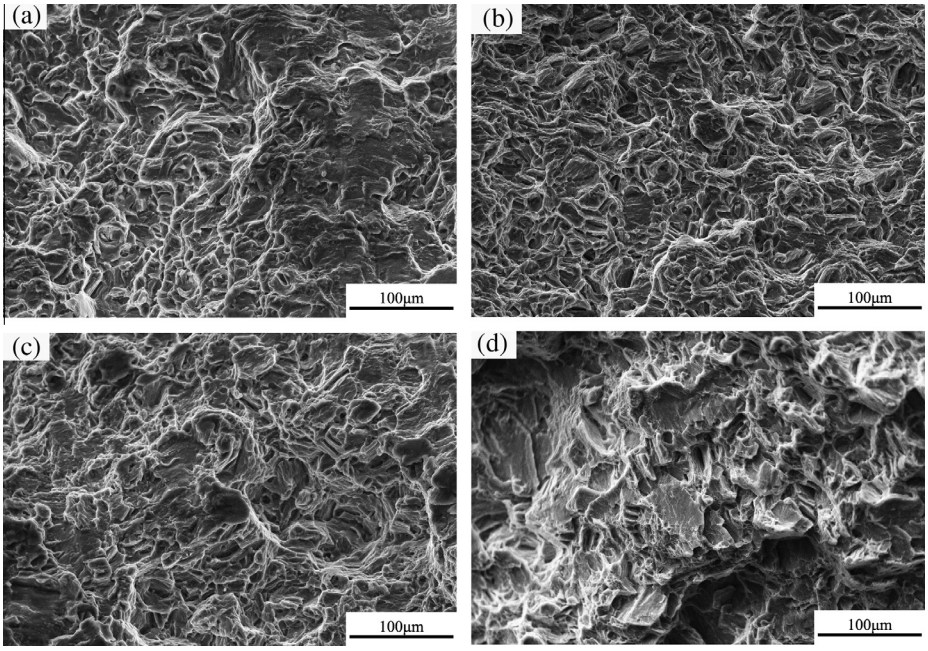

Fig. 5. The fracture surface of pre-compression specimens: (a) as-received, (b) PRC 1%, (c) PRC 3%, and (d) PRC 5%.

was observed between the flow stresses in samples subjected to PRC, owing to the difference of the volume fraction of twins for different PRC samples. Fig. 4 shows the strain hardening rate of PRC samples during inverse tension. Since there was no evident change of orientation in extruded magnesium alloy during tension along ED, the sample without pre-deformation did not exhibit any obvious work hardening. On the other hand, the PRC samples exhibited an apparent work hardening also depending on the amount on pre-compression experienced. Besides, it should be noted that the improvement of the peak strength might be related to twins subdividing and grain refinement.

The grain size of as-received, PRC 1%, PRC 3% and PRC 5% samples after inverse tension straining up to failure was 16.4 μm, 14.7 μm, 14.5 μm and 14.9 μm, respectively. Compared with the original data of 15.5 μm, the grain size slightly increased in the as-received materials after inverse tension. However, there were no obvious changes comparing with the PRC specimens. It can be concluded that the detwinning behavior had no significant effects on the grain size.

In Table 1, it is revealed that compared with as-received samples, the fracture elongation of samples subjected to different PRC levels improved mainly because of the softening orientation

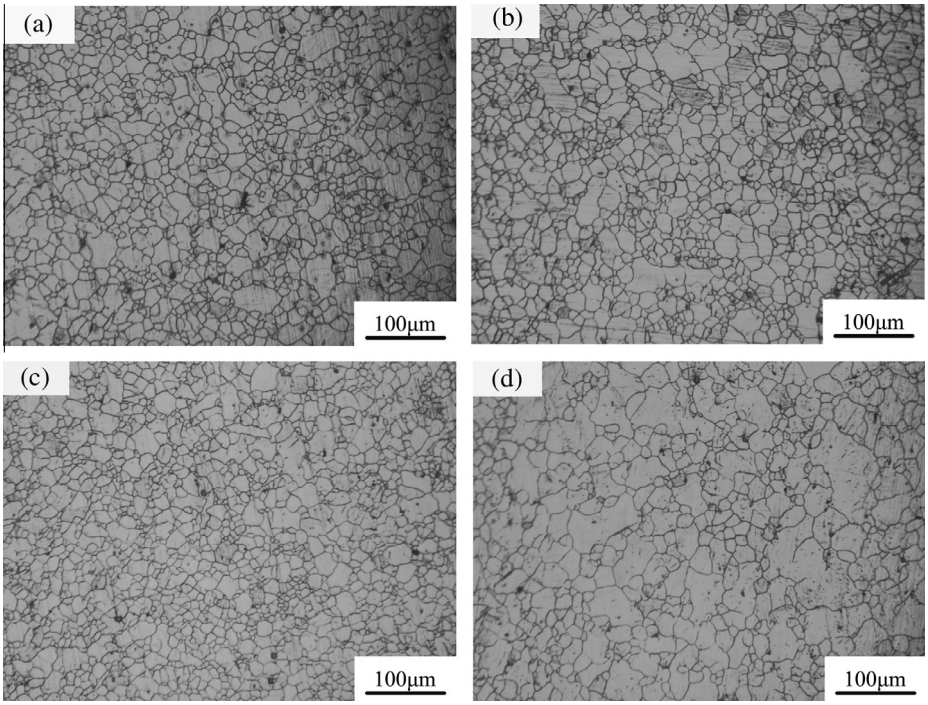

Fig. 6. The microstructure of pre-stretched samples at different degrees: (a) as-received, (b) PRS 1%, (c) PRS 3%, and (d) PRS 5%.

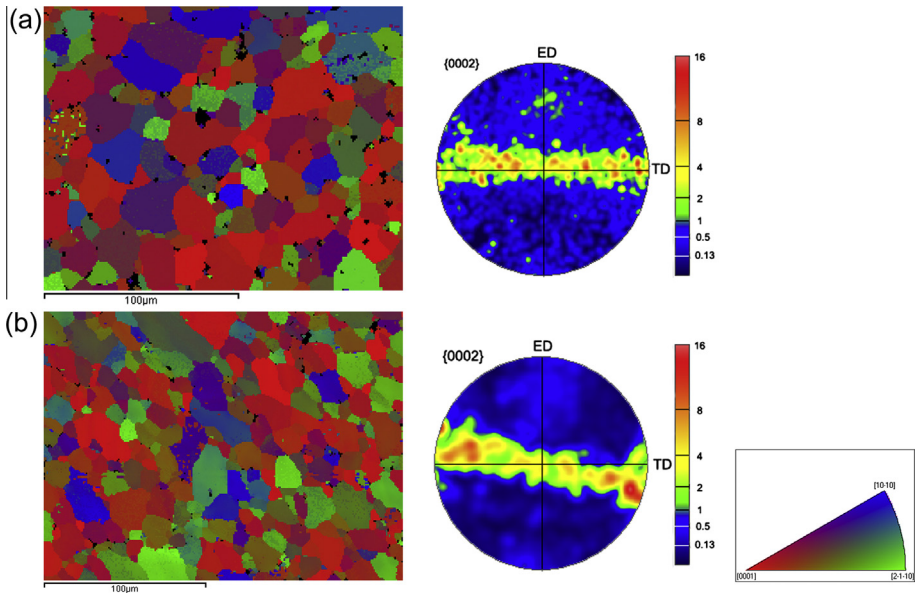

Fig. 7. (0002) pole figures and IPF maps of various samples: (a) as-received and (b) PRS 3%.

of grains after PRC. Jiang et al. [20] pointed out that the twins had a function of softening during the tension straining in an AM30 magnesium alloy since the orientation of twins had a contribution to the subsequent slip action. Furthermore, they also stated that the twinning-induced softening resulted in improvement of the alloy ductility. Since the softening effect depends on the volume fraction of the twins, the more produced twins the larger softening effect is visible. Barnett [21] also indicated the ductility improvement of AZ31 magnesium alloys by the {10−12} extensive twins. Accordingly, after pre-compression, the {10−12} twins had a softening effect since grain crystals rotated parallel to ED.

Fig. 5 depicts the fracture surface of different PRC specimens. The fracture surface of as-received specimen shows a number of local dimples along with some cleavage facets, implying a mixed ductile and cleavage facture (Fig. 5a). In contrast, in PRC specimens the number of dimples was more with respect to the samples without PRC. Moreover, it should be noted that the dimples in PRC 3% samples were deeper than those of PRC 1% samples. For PRC 5% specimens, tearing edges could be found in addition to the numerous deeper dimples. These aforementioned features are believed to be the evidence of an improvement of plasticity after pre-compression deformation. Therefore, it is supposed that accumulation of plastic

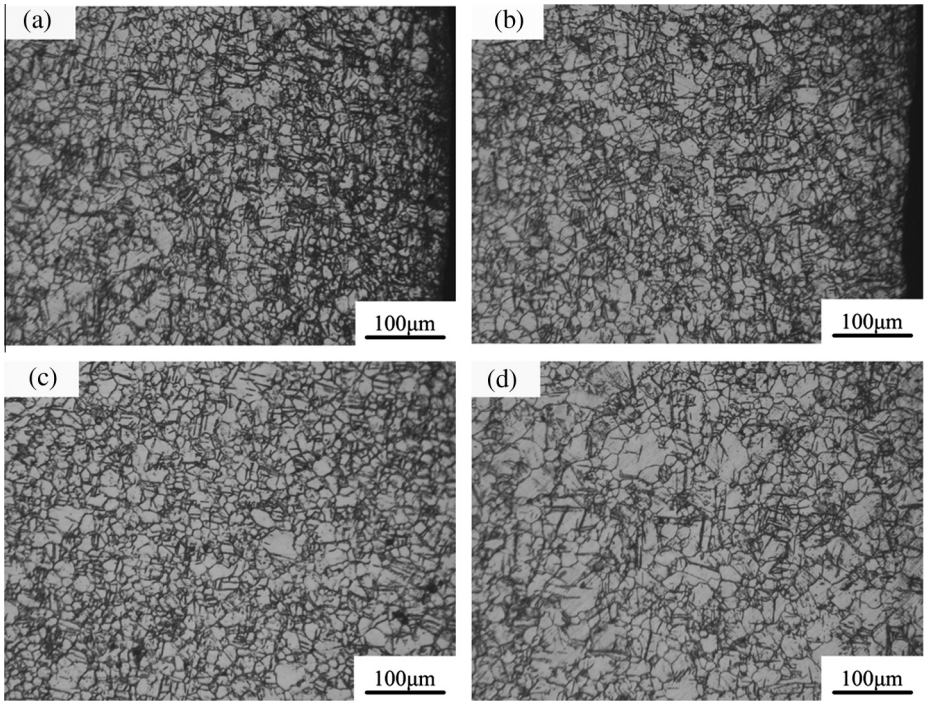

Fig. 8. The microstructure of AZ31 magnesium alloy inverse compression after pre-stretch with different degree: (a) as-received, (b) PRS 1%, (c) PRS 3%, and (d) PRS 5%.

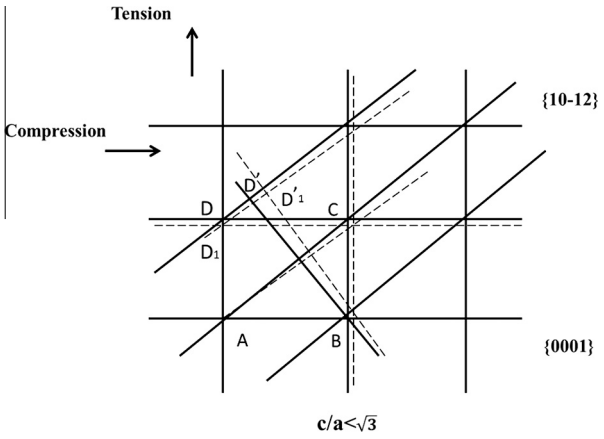

Fig. 9. Schematic diagram of movement of atoms in {10−12} plane induced by twins in AZ31 magnesium.

deformation in AZ31 alloy is promoted by inducing twinning–detwinning through pre-compression and, accordingly, improvement of fracture tensile elongation can be obtained.

3.3. Microstructure of pre-stretched samples

Fig. 6 shows the microstructure of AZ31 extruded alloy after pre-stretching with different deformation levels. As seen, after pre-stretching no evidence of twin was found and all microstructure was made of fairly homogeneous equiaxed grains. As well known, the {10−12} extension twinning only favored when the compression load was applied along ED or when tension was applied perpendicular to ED [22,23]. Otherwise, the slip would be the dominant deformation mechanism and no twinning would occur. Fig. 7 shows that the sample after pre-stretching to 3% expresses a basal texture substantially similar to the as-received one. He et al. [12] also reported that in an extruded AZ31 alloy the diffraction peak of various texture elements were kept consistent during tensile straining to 3% and even after tension fracture. Since the tensile process is mainly governed by slip, no evident orientation changes occurred during tension.

Fig. 8 shows the microstructure of various PRS samples (pre-stretched) after inverse compression. All the micrographs were taken close to fracture region. As seen, the volume fraction of twins decreased with increasing degree of pre-stretch deformation and also the twins were restrained by the PRS deformation.

During the inverse compression tests, the yield strength improved and the twins were restrained with increasing amount of pre-stretch, as shown in Fig. 1(b) and Table 1. Besides, the concave shape expressed by the stress–strain curves clearly showed that the dominant deformation mechanism during inverse compression after pre-stretch was still twinning.

Sheng et al. [24] reported that the c/a ratio of the HCP cells had dropped in the tensile part of fatigue cycles. Accordingly, the c/a ratio played a significant effect on twinning. The schematic diagram illustrating movement of atoms in {10−12} plane induced by twins is shown in Fig. 9. D is considered as an original position of an atom that has moved to D' through tangential strain induced by twinning. After pre-stretch, the c/a ratio decreases and D moves to D_1. After shear strain induced by twinning D_1 moves to D'_1, it can be seen that the distance of DD' is shorter than $D_1D'_1$. In other words, the distance of shear strain is longer after pre-stretch deformation and, thus, the resistance to active twinning increases at the same time. Accordingly, since the deformation is governed by twinning during inverse compression, higher values of yield strength are obtained. As the degree of pre-stretch increases, the c/a ratio declines more which leads to a higher resistance required to activate twinning. Hence, the yield strength increases with the increase of pre-stretch degree simultaneously.

4. Conclusions

The effects of twinning and detwinning on mechanical properties of AZ31 magnesium alloy were investigated by strain path changes after pre-compression and pre-stretching. The detwinning behavior occurred during inverse tension after pre-compression. Due to the softening orientation of {10−12} twins the yield strength decreased, while elongation to failure was improved. Besides, the softening effects were enhanced by the increase of pre-compression degree owing to presence of a larger volume fraction of twins. In the inverse compression test after pre-stretching, twinning was restrained and, moreover, the volume fraction of twins decreased as the degree of pre-stretching was developed. Since the c/a ratio of HCP cells decreased after pre-stretching, slipping and twining activation became more difficult, resulting in the increase of compressive yield strength.

Acknowledgements

This work is supported by Fundamental Research Funds for the Central Universities (No. CDJZR11130008). Lifei Wang is grateful for financial support of the China Scholarship Council (CSC).

References

[1] Zhang H, Huang GS, Roven HJ, Wang LF, Pan FS. Influence of different rolling routes on the microstructure evolution and properties of AZ31 magnesium alloy sheets. Mater Des 2013;50:667–73.
[2] Chino Y, Kimura K, Mabuchi M. Twinning behavior and deformation mechanisms of extruded AZ31 Mg alloy. Mater Sci Eng A 2008;486:481–8.
[3] Yasi JA, Hector LG, Trinkle DR. First-principles data for solid-solution strengthening of magnesium: from geometry and chemistry to properties. Acta Mater 2010;58:5704–13.
[4] Masoudpanah SM, Mahmudi R. The microstructure, tensile, and shear deformation behavior of an AZ31 magnesium alloy after extrusion and equal channel angular pressing. Mater Des 2010;31:3512–7.
[5] Knezevic M, Levinson A, Harris R, Mishra RK, Doherty RD, Kalidindi SR. Deformation twinning in AZ31: influence on strain hardening and texture evolution. Acta Mater 2010;58:6230–42.
[6] Yin DL, Wang JT, Liu JQ, Zhao X. On tension–compression yield asymmetry in an extruded Mg–3Al–1Zn alloy. J Alloys Compd 2009;478:789–95.
[7] Luo TJ, Yang YS, Tong WH, Duan QQ, Dong XG. Fatigue deformation characteristic of as-extruded AM30 magnesium alloy. Mater Des 2010;31:1617–21.
[8] Song B, Xin RL, Chen G, Zhang XY, Liu Q. Improving tensile and compressive properties of magnesium alloy plates by pre-cold rolling. Scripta Mater 2012;66:1061–4.
[9] Xin YC, Wang MY, Zeng Z, Nie MG, Liu Q. Strengthening and toughening of magnesium alloy by {10−12} extension twins. Scripta Mater 2012;66:25–8.
[10] Zhang H, Huang GS, Wang LF, Li JH. Improved formability of Mg–3Al–1Zn alloy by pre-stretching and annealing. Scripta Mater 2012;67:495–8.
[11] Wang YN, Huang JC. The role of twinning and detwinning in yielding behavior in hot-extruded Mg–Al–Zn alloy. Acta Mater 2007;55:897–905.
[12] He JJ, Liu TM, Xu S, Zhang Y. The effects of compressive pre-deformation on yield asymmetry in hot-extruded Mg–3Al–1Zn alloy. Mater Sci Eng A 2013;579:1–8.
[13] AQSIQ Standard GB/T 228-2002. Metallic materials-tensile testing at ambient temperature. General administration of quality supervision, inspection and quarantine of the People's Republic of China; 2002.
[14] AQSIQ Standard GB/T 7314-2005. Metallic materials-compressive testing at ambient temperature. General administration of quality supervision, inspection and quarantine of the People's Republic of China; 2005.
[15] Hong SG, Park SH, Lee CS. Role of {10−12} twinning characteristics in the deformation behavior of a polycrystalline magnesium alloy. Acta Mater 2010;58:5873–85.
[16] Lv CL, Liu TM, Liu DJ, Jiang S, Zeng W. Effect of heat treatment on tension–compression yield asymmetry of AZ80 magnesium alloy. Mater Des 2012;33:529–33.
[17] Lou XY, Li M, Boger RK, Agnew SR, Wagoner RH. Hardening evolution of AZ31B Mg sheet. Int J Plast 2007;23:44–86.
[18] Wu YJ, Zhu R, Wang JT, Jia WQ. Role of twinning and slip in cyclic deformation of extruded Mg–3%Al–1%Zn alloys. Scripta Mater 2010;63:1077–80.

[19] Wu W, Lee SY, Paradowska AM, Gao YF, Liaw PK. Twinning–detwinning behavior during fatigue-crack propagation in a wrought magnesium alloy AZ31B. Mater Sci Eng A 2012;556:278–86.
[20] Jiang L, Jonas JJ, Luo AA, Sachdev AK, Godet S. Twinning-induced softening in polycrystalline AM30 Mg alloy at moderate temperatures. Scripta Mater 2006;54:771–5.
[21] Barnett MR. Twinning and the ductility of magnesium alloys Part I: "Tension" twins. Mater Sci Eng A 2007;464:1–7.
[22] Proust G, Tomé CN, Jain A, Agnew SR. Modeling the effect of twinning and detwinning during strain-path changes of magnesium alloy AZ31. Int J Plast 2009;25:861–80.
[23] Chen WZ, Wang X, Hu LX, Wang E. Fabrication of ZK60 magnesium alloy thin sheets with improved ductility by cold rolling and annealing treatment. Mater Des 2012;40:319–23.
[24] Sheng GM, Zhang GT, Yan C. Research of bauschinger effect of AZ31 magnesium alloy. Rare Mater Eng 2011;40:616–9.